# Evidence of a Liquid-Liquid Phase Transition in Hot Dense Hydrogen

# Evidence of a Liquid-Liquid Phase Transition in Hot Dense Hydrogen

Vasily Dzyabura, Mohamed Zaghoo, and Isaac F. Silvera
Lyman Laboratory of Physics, Harvard University, Cambridge MA, 02138

We use pulsed-laser heating of hydrogen at static pressures in the megabar pressure region to search for the plasma phase transition (PPT) to liquid atomic metallic hydrogen. We heat our samples substantially above the melting line and observe a plateau in a temperature vs laser power curve that otherwise increases with power. This anomaly in the heating curve appears correlated with theoretical predictions for the PPT.

In 1935 Wigner and Huntington predicted that solid molecular hydrogen would become atomic and metallic when compressed to a pressure of 25 GPa in the ground state of the solid (1). Subsequent theoretical work showed that there could be two pathways to the metallic state: isothermal compression to the solid atomic metallic phase, also predicted to be a high temperature superconductor by Ashcroft (2), and the plasma phase transition (**PPT**), first discussed by Landau and Zeldovich (3). For hydrogen the PPT is predicted to be a first-order phase transition (involving molecular dissociation) to the atomic metallic liquid phase (for a recent short review see ref. (4)). In this contribution we shall discuss the phase diagram of hydrogen and our experiments designed to observe the PPT at static pressure **P** and high temperature **T**.

A mixed experimental/theoretical phase diagram of hydrogen is shown in Fig. 1. At the present time hydrogen has been pressurized to almost 400 GPa in diamond anvil cells (**DACs**) at room temperature and lower. Some years ago new high pressure, lower temperature phases were discovered and their phase lines determined. The lowest pressure phase has a hexagonal close packed (HCP) structure with all molecules in the spherically symmetric rotational ground state J=0. With increased pressure new phase lines were observed: the broken symmetry phase (BSP) (5), and the A-phases (6-8) for pure para-hydrogen, also referred to as I, II, and III for mixtures of ortho and para-hydrogen. These are insulating phases in which the spherically symmetric single-molecule states (at low pressure) becomes admixed with higher rotational states and thus have non-spherically symmetric distributions; the phase transitions involves orientational order of the molecules along crystalline directions. At still higher pressures (270 GPa) there was a recent claim of metallization of hydrogen (9) that has been refuted (10) or not supported by subsequent experiments (11, 12). However, there is recent evidence of a phase IV in the room temperature region above 200 GPa (12) that may be a semimetal (13).

Several years ago Bonev et al (14) carried out a theoretical study of the melting line as a function of pressure and predicted a maximum in this line. These calculations were only valid for high temperatures; it has been speculated that the melting line can be extended to higher pressures so that hydrogen would be liquid atomic metallic at multi-megabar pressures in the ground state in the limit that temperature goes to zero K (dotted line, Fig. 1). A calculation by Attaccalite and Sorella supports this extrapolation (15). Babaev et al (16) have discussed the possibility of two-component superconductivity (electrons and protons) for liquid atomic

hydrogen at high P and low T. At still higher pressures atomic hydrogen would again solidify. In support of these theoretical predictions for the melting line region of the phase diagram, Deemyad and Silvera (17) first observed the maximum in this curve using pulsed-laser heating. Melting line measurements were extended to higher pressures by Eremets and Troyan (18), and later confirmed by Subramanian et al (19), but not sufficiently high to confirm the extrapolation.

Scandolo (20) and others (14, 21-23) theoretically studied the higher temperature region above the melting line and found the PPT line. This line is not only a transition to conducting liquid atomic metallic hydrogen, but also a line of dissociation from molecular to atomic hydrogen. There are some differences in the calculations by various authors and we show the approximate range of theoretical results in Fig. 1with the two curves connected with horizontal bars. With increasing pressure the PPT line starts with a critical point and is predicted to be a first-order phase transition with a negative slope. Again, speculations suggest that the PPT line will intersect the melting line at higher pressures (dashed line). Thus, at still higher pressures hydrogen would melt directly from a molecular solid to an atomic liquid, according to these extrapolations.

There are reports of observation of electrical conductivity of hydrogen and deuterium at high pressure/temperature using reverberating shock-wave techniques where the P,T conditions are met for experimental lifetimes of ~100 ns. Weir, Mitchell, and Nellis (24) detected a large increase in electrical conductivity at 140 GPa (measured) and T~3000 K (calculated) to a metallic liquid, but the change was continuous; this measured point (Fig. 1) may be above the critical point. Fortov et al studied deuterium and observed a step in density at high P, T and "think" (25) that they have observed the PPT. They show a conductivity jump in a different sample, hydrogen (26). Hydrogen and deuterium are isoelectronic so we only expect a slight difference due to mass effects, which should not be very important at high temperatures. We plot the results of Fortov et al (for deuterium) in Fig. 1; they calculated the temperature from plasma models (we use pressure results from ref. (23)).

In this letter we offer new indirect evidence of the PPT observed with static pressures generated by a DAC, using a pulsed laser (Nd-Vanadate laser-wavelength1065 nm-with pulse times of order 100-200 ns) to heat to the sample. We focus on higher temperatures, above the melting line in the predicted region of the PPT, to collect evidence of the existence of this transition. Our experimental system was optimized for higher temperature studies; the lower temperature melting line data, extracted from the heating curves, are consistent with earlier measurements, but with larger uncertainties (see Supplementary Information, **SI**).

In our experiments hydrogen was cryogenically loaded in a DAC (27) that was removed from a cryostat to room temperature for laser heating. The diamond anvils with 100 μm diameter flats were beveled and were etched and coated with alumina to act as a hydrogen diffusion barrier, using atomic layer deposition (ALD). In order to laser heat the hydrogen, we embedded a platinum foil in the hydrogen to absorb the laser power and heat the hydrogen at its surface. Initial measurements started at pressures above 40 GPa; at these pressures hydrogen can diffuse into the Pt absorber and convert it to metallic platinum hydride (28, 29). We used rhenium gaskets with gasket holes as large as 50 μm diameter; the hole contained the platinum absorber (~20 μm square or round, 1.5 μm thick), surrounded by several ruby balls for pressure measurement, shown in Fig. 2. During loading in the liquid phase, the index of refraction of the sample was measured and confirmed to be that of liquid hydrogen. In total we had 6 loadings of the DAC, but only two runs yielded high temperature results, both showing plateaus to be discussed ahead; one of these had an indeterminate temperature offset.

Here we report on the last run (run2) with results from run1 in the SI. For run1 everything in the sample chamber was coated by alumina using ALD. This is interesting because the alumina diffusion barrier should prevent the transformation of Pt to platinum hydride, so that our absorber in run1 should be Pt, while in run2 the absorber was unprotected and would convert to platinum hydride. However, the coating on the absorber leads to a positive offset in the measured temperature that could not be determined (see SI). The first run terminated unexpectedly when the tungsten carbide plate supporting an anvil failed. Run2 was terminated when conditions in the sample region deteriorated so that we could not obtain reliable results.

Pressures were determined both from the ruby fluorescence using the pressure scale of Chijioke et al (30) and the diamond phonon Raman edge using the calibration of Akahama et al (31); these two pressure determinations were in reasonable agreement with each other. Pressure was measured at room temperature. The uncertainty in pressure determination was no more than 2-3 GPa at the highest pressures. Such uncertainties are not important for the present investigation and we do not plot pressure error bars in our data. Although one can expect the pressure to increase with increasing temperature (thermal pressure) in our quasi-isochoric sample chamber, we believe that our pressures are reasonably representative due to the negative slope at the phase transitions: the pressure decreases as the temperature crosses the transition line (as predicted by the Clapeyron-Clausius equation) and can help compensate for the thermal pressure increase.

We determine the peak temperature of the absorber, and thus that of the contacting hydrogen, from the time-averaged spectral irradiance of the absorber surface by doing a two-parameter fit (emissivity and temperature) to the Planck blackbody (**BB**) curve. We correct for time dependent temperature changes due to the pulsed nature of the heating (32, 33). In this method, due to the temporal nature of the heating pulse, the spectral irradiance is slightly distorted from the BB curve for a fixed temperature. The observed irradiance is fit to a BB curve yielding a temperature called the Planck temperature. The analysis correlates the peak temperature of the thermal pulse to the measured Planck temperature. Reference (32) used a geometry of a semi-infinite heated plane for the analysis; here we implemented a finite element analysis (FEA) using the cell geometry to develop a correlation table. In a parallel analysis we used the information from thermoreflectivity (discussed below) to determine the shape of the temperature pulse and develop a correlation table; both methods yielded the same result. The measured spectral region of the irradiance is at a longer wavelength than in the analysis of refs. (32) and (33); this has been taken into account in our analysis. We have carried out a FEA of the melted region of hydrogen and find the melted volume to be a thin film in contact with the absorber with a thickness in the range of 0.5 to 1 micron.

The optical set-up is shown in the SI. Briefly, the power of the pulsed-laser could be changed by rotating a half-wave plate (HWP) to vary the angle of polarization incident on a corner cube beam-splitter. This laser is defocused at the absorber so that it is filled with the peak of the Gaussian beam to provide a reasonably uniform illumination. The maximum average power was ~1 Watt. The laser beam is focused beyond the absorber to avoid focusing in the diamond which can damage the anvil, but most of the power fell on the absorber whose linear dimensions were ~20 microns. Light from the absorber is collected with an imaging Schwarzschild objective, spatially filtered to observe a 20 μm diameter spot that is imaged on the slits of a prism spectrometer, and detected by an InGaAs diode array sensitive from 0.9 to 1.7 microns. Fitting to the BB curve was done in the 1.4 to 1.62 micron infrared region. The sample could be observed on a video CCD, simultaneously. The system had a shutter and automated

HWP rotator so that a curve of T versus average pulse power could be measured (a heating curve) under computer control. A CW laser beam could shine on the absorber region, collinear with the pulsed laser, for measuring ruby fluorescence as well as reflectivity, using a grating spectrometer and visible CCD detector, respectively.

In principle a heating curve should be a monotonically increasing curve of temperature vs laser power without singularities. However, one can expect a change in the slope of the curve or a plateau when the sample undergoes a phase transition. An FEA by Montoya and Goncharov (34) has shown that the melting curve should at best show a change of slope, although plateaus have been observed in many experiments. An FEA analysis by Geballe and Jeanloz (35) shows that plateaus in heating curves may also result from a change of reflectivity at a transition.

The raw spectra not only contained the incandescent BB radiation used to determine the temperature, but also the Raman phonon and fluorescence spectrum from the diamond. These spectral contributions could be separated (see SI), as the Raman intensity is linear with laser power and the BB is nonlinear. The time required to measure a single spectrum ranged from 30 to 0.1 seconds, depending on the temperature, and for a full heating curve about 30 minutes. Due to the low duty-cycle of pulsed-laser heating (repetition rate of 20 kHz with ~100 ns pulses), our sensitivity for determining T from BB radiation started at ~800 K. Measurement times were limited to about 30 minutes/heating-curve due to the temporal instability of the system. Essentially the sample was imaged on the spatial filter and the image would slowly drift. This image was not continuously monitored, but sampled by the video CCD. As a consequence of these problems, for this detection system the signal-to-noise was quite low for low temperatures where nonlinear contributions are quite small. Thus, we could not reliably resolve plateaus at the melting line, as did Deemyad and Silvera (17), but rather detected a change of slope in the heating curves (see SI). The narrow-bandpass filter measurements of ref. (17) were at longer wavelengths that would not have been contaminated by diamond Raman background.

Figure 3 shows heating curves at 119 GPa and 125 GPa typical of our data. While the data is quite noisy at low temperature, at elevated temperatures the S/N ratio is high. In general the temperature rises with laser power; the high temperature plateau is quite distinct, and the temperature of the plateau was reproducible at each pressure. Note that at the plateaus the putative error bars are large; however this corresponds to increased temperature fluctuations rather than the noise of the detection system. The melting line is at a substantially lower temperature and due to the low signal-to-noise ratio we observe a change of slope (see SI for results). Data for the heating curve plateaus are plotted in Fig. 1 and correlate with the theoretical predictions (14, 20-23), demonstrating the negative slope, while the existence of the transition to plateaus implies a phase transition. Thus, we believe that the high temperature plateau is a signature of the phase transition to the PPT. A plateau was also observed in run1 at 155 GPa (see SI). In run2 as the pressure was increased the gasket hole closed down and shifted so that the viewable area of the absorber decreased and the heating curves did not display well-defined plateaus. We made an effort to understand this behavior by viewing the absorber when hot. Throughout the experiment we were very conservative, not heating the absorber to temperatures much above the plateau. At this point we decided to heat above 2000 K so that the glow of the absorber was visible with our video CCD monitor. When the absorber was imaged while hot, it displayed three distinct hot spots (see SI). Thus, we attribute the absence of the plateau to non-uniform heating and averaging out of the plateau. A possible explanation for this is that the absorber deformed with increasing pressure so that it was non-uniformly heated. At the end of

the run, while releasing the load, the gasket hole completely closed as the hydrogen escaped, enclosing the absorber, precluding further high-resolution analysis.

A secondary measurement is the reflectivity of the absorber/sample. Whereas one expects a sharp change in transmission of hot hydrogen at the PPT, reflection is less sensitive. The challenge here is the following. First of all, if metallic hydrogen is a reasonable liquid metal, it will have a reasonably high reflectivity and a small penetration depth for light, so that for T greater than the transition temperature to the PPT, hydrogen, not the absorber, will dominate the reflection. However, platinum hydride is a reasonably good metal so that the change of reflectivity at the PPT may be small. This problem is exacerbated because the reflectivity of most metals is temperature dependent, so one must observe a small change on a large slope with changing temperature, or a change of slope corresponding to different temperature dependencies of hydrogen and platinum hydride reflectivities. In the geometry used in our experiment we could shine a visible CW laser beam on the sample, collinear with the pulsed laser. In this case, we do not measure specular reflection but diffuse reflection, as the small mirror of the Schwarzschild objective substantially blocks the specular component. Nevertheless, the diffuse light signal is quite strong, due to surface roughness of the absorber, while there can be a small specular contribution to the signal due to the cupping of the diamond culet flats at high pressure. This signal displays strong temperature dependence, shown in Fig. 4. We clearly see the time resolved heating and cooling of the sample, and this enables a determination of the thermal time constant of the surface. This information was used in the fitting algorithm used to calculate the relationship between the Planck and peak temperature, discussed above. We did not perform systematic measurements on reflectance vs. temperature due to mechanical stability problems for all pressure points. Our preliminary data shows a change in intensity of reflected light in the plateau region (see SI), consistent with either darkening of the sample or a change in the diffuse/specular ratio towards weaker diffuse and stronger specular reflection.

In conclusion we have demonstrated that with our new techniques (diamond preparation), hydrogen at high static pressures can be studied well above the melting line where plateaus have been observed in heating curves. In such studies, plateaus are associated with phase transitions and we have determined the temperature of the plateaus as a function of pressure. The negative slope of the temperature of the plateaus as a function of pressure is the expected dependence for the PPT. The sizeable plateaus that we have observed are indicative of a phase transition with a large heat of transformation or abrupt change of reflectivity, as one might expect for the molecular dissociation that transpires at the PPT (23). At the current time all evidence of the PPT has been indirect: Weir et al (24) demonstrate conductivity, but no phase transition; Fortov et al (25) show a density change for deuterium, but do not measure conductivity in their deuterium sample; their data, as ours, presents evidence of a phase transition. Our current measurement demonstrates a close correlation between a plateau demonstrative of a phase transition and theoretical predictions for the PPT. Our static pressure method has great promise to provide rigorous evidence of metallization from optical properties of the sample, complementing our present observations. There are some uncertainties that accrue in this challenging experimental region. We plan to further eliminate the possibility that the observed changes arise from the absorber. We believe that the absorbers in run1 and run2 were platinum and platinum hydride, respectively. New experiments are being developed with different absorber materials and to measure the transmission of the hot dense hydrogen.

We thank Evgeniya Zarechnaya for aid in preparing the experiment and Eran Sterer, Goutam Dev Mukherjee, and Bill Nellis for discussions. The NSF, grant DMR-0804378 and the

DOE Stockpile Stewardship Academic Alliance program, grant DE-FG52-10NA29656 supported this research. Preparation of diamond surfaces was performed at the Center for Nanoscale Systems (CNS), which is supported by the NSF award no. ECS-0335765. CNS is part of Harvard University.

## References

1. Wigner E & Huntington HB (1935) On the Possibility of a Metallic Modification of Hydrogen. *J. Chem. Phys.* 3:764-770.
2. Ashcroft NW (1968) Metallic Hydrogen: A High Temperature Superconductor? *Phys. Rev. Lett.* 21(26):1748-1749.
3. Landau LD & Zeldovich YB (1943) On the relation between the liquid and the gaseous states of metals. *Acta Physico-Chimica U.R.S.S.* 18:380.
4. Silvera IF (2010) The insulator-metal transition in hydrogen. *Proc. of the National Academy of Sciences* 107:12743-12744.
5. Silvera IF & Wijngaarden RJ (1981) New Low Temperature Phase of Molecular Deuterium at Ultra High Pressure. *Phys. Rev. Lett.* 47:39-42.
6. Lorenzana HE, Silvera IF, & Goettel KA (1989) Evidence for a Structural Phase Transition in Solid Hydrogen at Megabar Pressures. *Phys. Rev. Lett.* **63**:2080-2083.
7. Hemley RJ & Mao HK (1988) Phase Transition in Solid Molecular Hydrogen at Ultrahigh Pressures. *Phys. Rev. Lett.* 61:857-860.
8. Lorenzana HE, Silvera IF, & Goettel KA (1990) Orientational Phase Transitions in Hydrogen at Megabar Pressures. *Phys. Rev. Lett.* 64:1939-1942.
9. Eremets MI & Troyan IA (2011) Conductive Dense Hydrogen. *Nature Materials* 10:927-931.
10. Nellis WJ, Ruoff AL, & Silvera IF (2012) Has Metallic Hydrogen Been Made in a Diamond Anvil Cell? *arXiv:1201.0407v1*.
11. Zha C-S, Liu Z, & Hemley RJ (2012) Synchrotron Infrared Measurements of Dense Hydrogen to 360 GPa. *Phys. Rev. Lett.* 108(14):146402-146407.
12. Howie RT, Guillaume CL, T.Scheler, Goncharov AF, & Gregoryanz E (2012) Mixed molecular and atomic phase of dense hydrogen. *Phys. Rev. Lett.* 108:125501.
13. Lebegue S, *et al.* (2012) Semimetallic dense hydrogen above 260 GPa. *Proc. of the National Academy of Sciences* 109:9766-9769.
14. Bonev SA, Schwegler E, Ogitsu T, & Galli G (2004) A quantum fluid of metallic hydrogen suggested by first-principles calculations. *Nature* 431:669-672.
15. Attaccalite C & Sorella S (2008) Stable Liquid Hydrogen at High Pressure by a Novel *Ab Initio* Molecular-dynamics Calculation. *Phys. Rev. Lett.* 100:114501.
16. Babaev E, Sudbo A, & Ashcroft NW (2004) A superconductor to superfluid transition in liquid metallic hydrogen. *Nature* 431:666-668.
17. Deemyad S & Silvera IF (2008) Melting Line of Hydrogen at High Pressures. *Phys. Rev. Lett.* 100:155701.
18. Eremets MI & Trojan IA (2009) Evidence of Maximum in the Melting Curve of Hydrogen at Megabar Pressures. *JETP Letters* 89:174-179.

19. Subramanian N, Goncharov AF, Struzhkin VV, Somayazulu M, & Hemley RJ (2011) Bonding changes in hot fluid hydrogen at megabar pressures. *Proc. of the National Academy of Sciences* 108:6014-6019.
20. Scandolo S (2003) Liquid-liquid phase transitions in compressed hydrogen from first-principles simulations. *Proc. Nat. Acad. of Sciences* 100:3051-3053.
21. Lorenzen W, Holst B, & Redmer R (2010) First-order liquid-liquid phase transition in dense hydrogen. *Phys. Rev. B* 82:195107.
22. Morales MA, Pierleoni C, Schwegler E, & Ceperley DM (2010) Evidence for a first order liquid-liquid transition in high pressure hydrogen from ab-initio simulations. *PNAS* 107:1299-12803.
23. Tamblyn I & Bonev SA (2010) Structure and Phase Boundaries of Compressed Liquid Hydrogen. *Phys. Rev. Lett.* 104:065702-065704.
24. Weir ST, Mitchell AC, & Nellis WJ (1996) Metallization of Fluid Molecular Hydrogen at 140 GPa (1.4 Mbar). *Phys. Rev. Lett.* 76:1860-1863.
25. Fortov VE, *et al.* (2007) Phase Transition in a Strongly Nonideal Deuterium Plasma Generated by Quasi-Isentropical Compression at Megabar Pressures. *Phys. Rev. Lett.* 99:185001-185004.
26. Fortov VE & al. e (2003) Pressure-Produced Ionization of Nonideal Plasma in a Megabar Range of Dynamic Pressures. *JETP* 97:261-278.
27. Silvera IF & Wijngaarden RJ (1985) Diamond Anvil Cell and Cryostat for Low Temperature Optical Studies. *Rev. Sci. Instrum.* 56:121.
28. Hirao N, Hiroshi F, Yasuo O, Kenichi T, & K.Takumi ( 2008) Synthesis and structure of new platinum hydrides at high pressure. in *Int. Symp. on metal-hydrogen systems* (Reykjavik, Iceland).
29. Degtyareva O, Proctor JE, Guillaume CL, Gregoryanz E, & Hanfland M (2009) Formation of transition metal hydrides at high pressures. *Solid State Communications* 149:1583-1586.
30. Chijioke A, Nellis WJ, Soldatov A, & Silvera IF (2005) The Ruby Pressure Standard to 150 GPa. *J. Appl. Phys.* 98:114905.
31. Akahama Y & Kawamura H (2006) Pressure calibration of diamond anvil Raman gauge to 310 GPa. *J. Appl. Phys.* 100(043516).
32. Rekhi S, Tempere J, & Silvera IF (2003) Temperature determination for nanosecond pulsed laser heating. *Rev. Sci. Inst.* 74:3820-3825.
33. Deemyad S, *et al.* (2005) Pulsed Laser Heating and Temperature Determination in a Diamond Anvil Cell. *Rev. Sci. Instruments* 76:125104.
34. Montoya J & Goncharov AF (2012) Finite element calculations of the time dependent thermal fluxes in the laser-heated diamond anvil cell. *Journal of applied physics* 111:112617.
35. Geballe Z & Jeanloz R (2012) Finite element calculations of the time dependent thermal fluxes in the laser-heated diamond anvil cell. *Journal of applied physics* 111:123518.

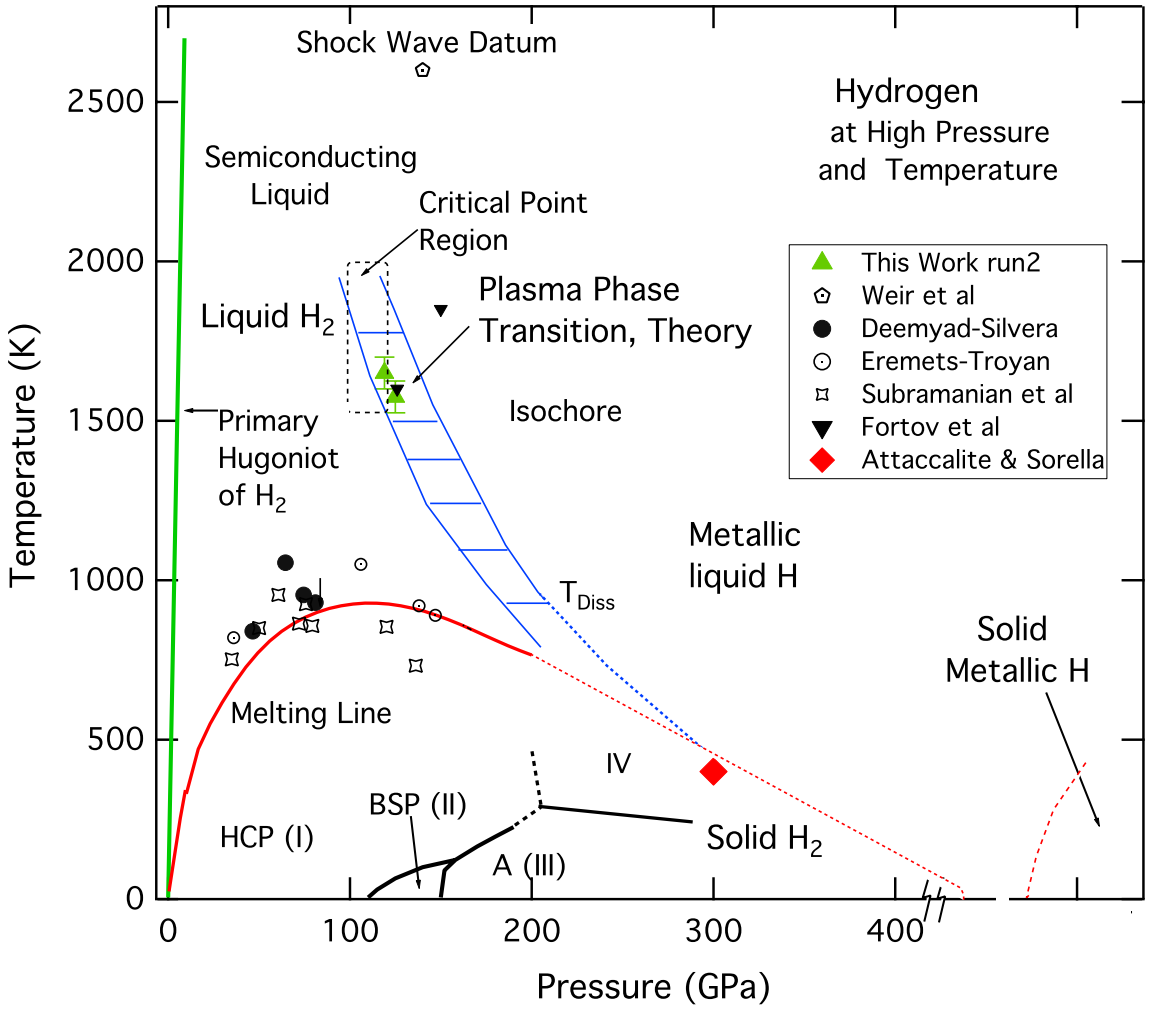


Figure 1. A mixed experimental/theoretical phase diagram of hydrogen, showing the melting line and PPT data, as well as the theoretical curves for these lines. For the PPT we show a range of curves resulting from recent calculations (14, 20-23) by the two curves connected with horizontal bars. The predicted position of critical point also varies with calculation, roughly indicated by the dotted rectangular box. We show our data in the region of the PPT as well as that of others. The two data points for Fortov et al (for deuterium) are in the molecular and the atomic liquid phases.

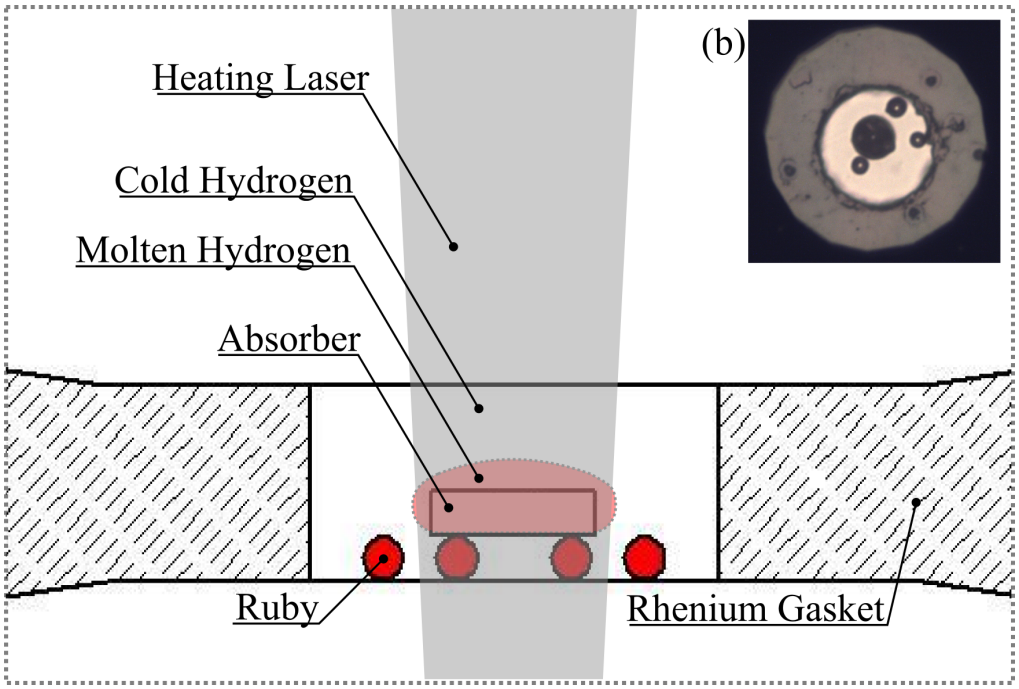


Figure 2. The heart of the DAC showing the absorber and ruby balls used for pressure measurement. The absorber is mounted on ruby balls to insulate from the high thermal conductivity diamonds. The diamonds are protected from hydrogen diffusion by a layer of alumina built up by low temperature ALD (not shown). The inset (b) shows a mounted gasket before pressurization

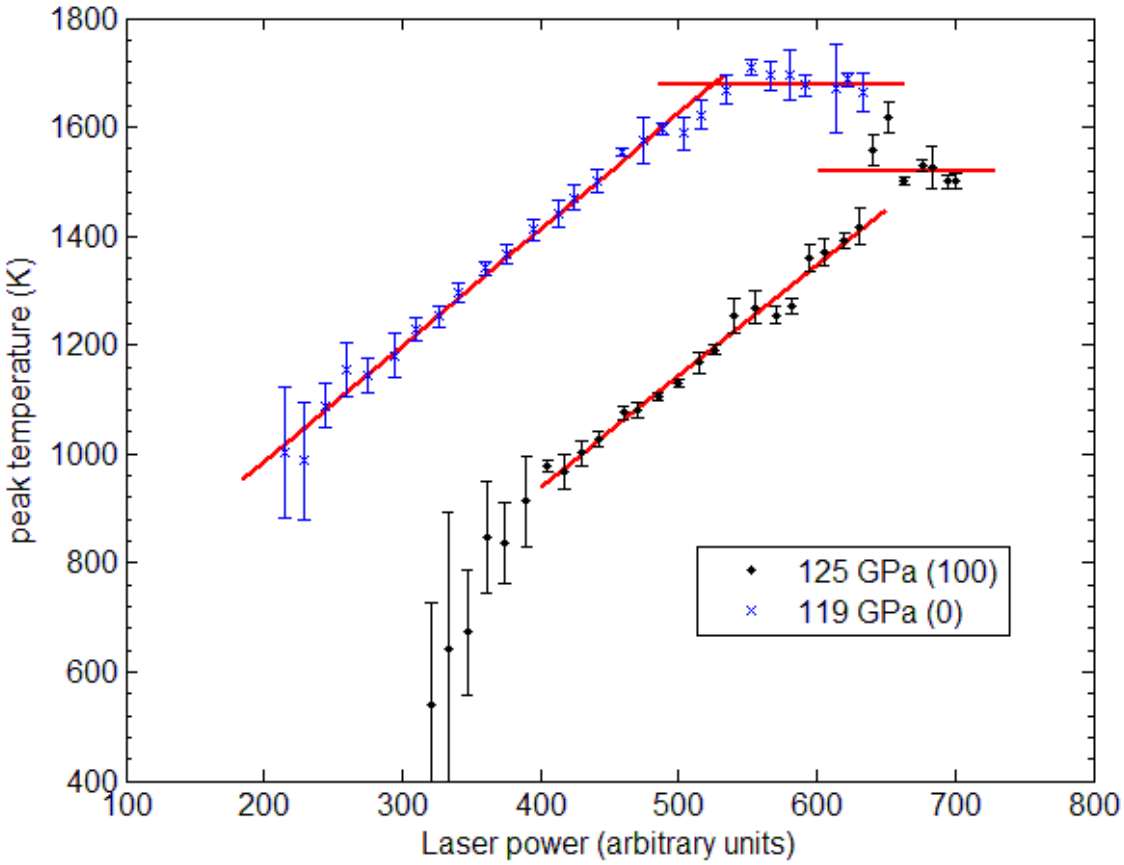


Figure 3. Plots of the peak temperature versus average laser power showing the rise in temperature and the plateaus for measurements at 119 GPa and 125 GPa. For every laser power, four spectra were taken and processed independently; the noise bars represent the standard deviation of the fitted temperatures. The straight lines are guides to the eye. The curves have been offset along the x-axis for clarity; the offsets of power are in parentheses in the legend.

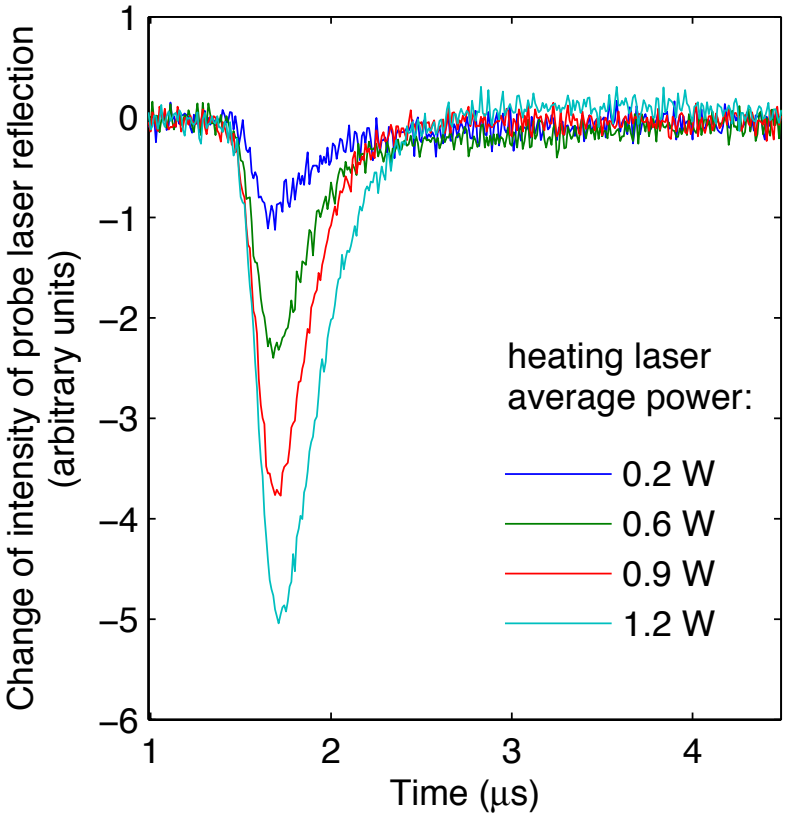


Figure 4. The change of the diffuse reflectivity of the absorber for a CW visible laser beam during a heating pulse (specular components may be involved due to cupping of the diamonds). This was measured for four different heating laser powers. This observation of temperature dependent reflectivity decrease and recovery allows one to estimate the thermal time constant of the system.